

# Utilizing the Potential of Solid Waste (Fly Ash and Bottom Ash) from Sumatera's Coal Power Plants for Innovative Geopolymer Concrete

Ferian Anggara<sup>1,2</sup>, Vincent Sutresno Hadi Sujoto<sup>2,3,4</sup>, Hotden Manurung<sup>3</sup>, Dea Anisa Ayu Besari<sup>2,3</sup>, Wali Al Hasunah<sup>5</sup>, Resti Natalia Ginting<sup>5</sup>, Febriansyah Febriansyah<sup>5</sup>, Amelia Andriani<sup>3,4</sup>, Robertus Dhimas Dhewangga Putra<sup>2,6</sup>, Januarti Jaya Ekaputri<sup>7</sup>, Himawan Tri Bayu Murti Petrus<sup>2,3\*</sup>

<sup>1</sup> Department of Geological Engineering, Faculty of Engineering, Universitas Gadjah Mada, Jl. Grafika 2., 55281 Yogyakarta, Indonesia

<sup>2</sup> Unconventional Geo-Resources Research Group, Faculty of Engineering, Universitas Gadjah Mada, Jl. Grafika 2., 55281 Yogyakarta, Indonesia

<sup>3</sup> Department of Chemical Engineering, Faculty of Engineering, Universitas Gadjah Mada, Jl. Grafika 2., 55281 Yogyakarta, Indonesia

<sup>4</sup> Research Center for Mineral Technology, Research Organization for Nanotechnology and Materials, National Research and Innovation Agency (BRIN), Kawasan Sains Iskandar Zulkarnain, Jl. Sutami KM 15, Tanjung Bintang, 35361 Lampung Selatan, Indonesia

<sup>5</sup> PT. Bukit Asam Tbk., Jl. Parigi No.1, 31716 Tanjung Enim, Sumatera Selatan, Indonesia

<sup>6</sup> Department of Mechanical Engineering, Faculty of Engineering, Universitas Gadjah Mada, Jl. Grafika 2., 55281 Yogyakarta, Indonesia

<sup>7</sup> Departement of Civil Engineering, Faculty of Engineering, Institut Teknologi Sepuluh Nopember, 2nd Floor ITS Campus, Keputih, Sukolilo, 60111 Surabaya, East Java, Indonesia

\* Corresponding author, e-mail: [bayupetrus@ugm.ac.id](mailto:bayupetrus@ugm.ac.id)

Received: 03 January 2026, Accepted: 17 April 2026, Published online: 19 May 2026

## Abstract

Indonesia, with its vast coal reserves, relies heavily on coal-fired power plants, which supply around 50% of the nation's energy needs. These operations generate large quantities of fly ash and bottom ash (FABA) as residual byproducts, posing environmental and health risks if not properly managed. Geopolymer technology offers a sustainable pathway to convert these wastes into value-added construction materials. This study investigates the utilization of FABA from a Sumatera-based coal power plant as aluminosilicate precursors for geopolymer concrete synthesis. Sodium hydroxide and sodium silicate were employed as alkaline activators, and the effects of fly ash to bottom ash ratio, NaOH concentration, and curing temperature on compressive strength were systematically evaluated. The results demonstrate that FABA can be effectively applied in geopolymer production. The optimum formulation achieved a compressive strength of 29.4 MPa using 100% fly ash, 8 M NaOH, and curing at 90 °C. Increasing the NaOH concentration beyond 8 M did not improve compressive strength, while higher curing temperatures enhanced strength development but also induced microcrack formation. These findings confirm that FABA-based geopolymers provide a technically viable and environmentally sustainable alternative to conventional cementitious materials, supporting circular economy strategies for coal ash management in Indonesia.

## Keywords

fly ash-bottom ash (FABA), geopolymer concrete, alkali-activated materials, curing temperature, circular economy

## 1 Introduction

Coal remains one of the dominant global energy sources, with coal-fired power plants contributing approximately 50% of Indonesia's total energy consumption in 2016 [1]. During the same year, Indonesia's coal production reached 28,457.29 million tons [2], resulting in the generation of large quantities of coal fly ash and bottom ash, which pose serious handling and environmental

challenges [3, 4]. Recent studies have explored various utilization pathways for these coal combustion by-products, including their application in pavers, geopolymer concrete [5, 6], and the recovery of valuable elements such as rare earth elements (REEs) [7, 8]. Among these approaches, the use of fly ash and bottom ash as geopolymer concrete has gained increasing attention, particularly

as a sustainable alternative to Portland cement in developing regions of Indonesia.

Unlike Portland cement, which relies on energy-intensive limestone calcination and generates substantial CO<sub>2</sub> emissions, geopolymer production offers a lower-energy process with significantly reduced CO<sub>2</sub> emissions [9, 10]. Human activities in the industrial and energy sectors are major contributors to environmental degradation and climate change. Global warming has intensified since 1880, with average global temperatures increasing by 0.08 °C per decade, accelerating to 0.18 °C per decade since 1981 [11]. This rapid warming is primarily driven by greenhouse gas (GHG) emissions from anthropogenic activities, which enhance the greenhouse effect by trapping heat in the atmosphere.

Geopolymers have emerged as promising substitutes for Portland cement due to their lower energy consumption and reduced CO<sub>2</sub> emissions during production [12]. Compared to Portland cement concrete, geopolymers can exhibit high compressive strength and low shrinkage, as well as better acid resistance, thermal stability, fire resistance, and the ability to immobilize heavy metals than Portland cement concrete [13]. Geopolymers are synthesized through geopolymerization, a chemical reaction between aluminosilicate precursors and alkaline activators, forming alkaline-bonded ceramic materials [12]. Their general chemical composition is expressed as:  $M_n \{-(\text{SiO}_2)_z - \text{AlO}_2\}_n \cdot w\text{H}_2\text{O}$ , where  $M$  represents alkali cations such as Na<sup>+</sup> or K<sup>+</sup>, and the Si/Al atomic ratio ( $z = 1-3$ ) governs the formation of amorphous to semicrystalline structures, including poly(sialate), poly(sialate-siloxo) and poly(sialate-disiloxo) frameworks [14]. Geopolymer concrete can be produced using either dry (monolithic or water-added) or wet (two-part) methods, depending on the interaction between aluminosilicate sources and alkaline solutions. The geopolymer system consists of three main components: aluminosilicate raw materials, fillers and geopolymer liquor containing alkaline hydroxide as well as silicate solutions that function as activators and binders [15].

Alkali-activated materials (AAMs) are a broad class of inorganic binders synthesized through the reaction between solid aluminosilicate precursors and alkaline activators. Within this system, geopolymers represent a specific subgroup of AAMs characterized by a three-dimensional aluminosilicate network with low calcium content and predominantly amorphous to semicrystalline structures [16, 17]. In geopolymer systems, the precursor refers to the solid aluminosilicate source (e.g., fly ash, bottom ash, metakaolin

or slag) that provides reactive Si and Al species, while the activator denotes the alkaline solution (commonly sodium or potassium hydroxide and silicate solutions) that dissolves and activates the precursor, initiating geopolymerization reactions. Coal fly ash (FA) and bottom ash (BA) are particularly suitable precursors due to their high aluminosilicate content. Prior research has shown that coal ash-based geopolymers exhibit favorable mechanical properties and polymerization behavior, supporting their potential as cementitious materials [15]. This study aims to synthesize geopolymers using coal fly ash and bottom ash sourced from coal-fired power plants in Sumatera. The effects of ash mixing ratio, alkaline activator concentration, and curing temperature on compressive strength were systematically investigated to develop environmentally friendly geopolymer concrete. In addition, Fourier transform infrared spectroscopy (FTIR) correlation data were employed to evaluate the progression of geopolymerization.

Despite extensive studies on fly ash-based geopolymers, the utilization of combined fly ash and bottom ash (FABA) systems remains insufficiently explored, particularly with respect to their integrated effects on mechanical performance and geopolymerization behavior. Most existing studies focus on single ash sources or limited processing parameters, while the combined influence of fly ash to bottom ash ratio, alkaline activator concentration, and curing temperature has not been systematically evaluated, especially for coal combustion residues from Sumatera.

In addition, the effects of local ash characteristics, such as unburned carbon content and mineralogical composition, on geopolymer performance remain poorly understood, despite their critical role in governing reactivity and mechanical properties. This gap limits the consistent reuse of FABA in geopolymer systems and reduces confidence in its broader application as a construction material.

Accordingly, this study aims to investigate the feasibility of utilizing Sumatera-derived FABA as aluminosilicate precursors for geopolymer concrete, systematically evaluate the effects of FA:BA mass ratio, NaOH concentration and curing temperature on compressive strength, as well as elucidate the relationship between geopolymerization degree and mechanical performance using FTIR-based correlation analysis. From an application perspective, the results address key challenges related to coal ash waste accumulation, heterogeneous material quality, and inconsistent mechanical performance, providing practical guidance for the sustainable reuse of FABA in construction materials within a circular economy framework.

## 2 Materials and methods

### 2.1 Raw material preparation

Fly ash and bottom ash were collected from three coal-fired power plants in South Sumatera, Indonesia: PLTU Lampung (LA), PLTU Tanjung Enim (EN), and PLTU BPI (BPI). All plants operate using a fluidized circulating bed system at a boiler temperature of approximately 850 °C. Fly ash samples were obtained from silos and landfills, while bottom ash samples were collected from ash ponds and landfills. Sodium hydroxide and sodium silicate (water glass) supplied by PT Brataco Chemical were used as alkaline activators. Commercial sodium silicate solution (water glass, analytical grade) containing approximately 30 wt.% SiO<sub>2</sub> and 9 wt.% Na<sub>2</sub>O with a SiO<sub>2</sub>/Na<sub>2</sub>O modulus ratio of 3.2 was used as the alkaline activator. Prior to use, both ashes were oven-dried at 120 °C for 4 h. Fly ash was sieved to particle sizes smaller than 200 mesh (< 75 μm), while bottom ash was used in particle sizes ranging from 20 mesh (≈ 850 μm) to coarse fractions.

### 2.2 Methodology

The alkaline activator was prepared by mixing sodium hydroxide solution and sodium silicate at a volume ratio of 1:1. Sodium hydroxide concentrations of 6 M, 8 M and 10 M were employed. The activator solutions were homogenized using a magnetic stirrer for 30 min prior to use.

Geopolymer pastes were prepared by mixing fly ash and bottom ash with the alkaline activator using a laboratory-scale planetary mixer to ensure homogeneous mixing. The FA:BA ratios were set at 100:0, 90:10, and 80:20. Depending on the mixture composition and workability, 80–100 mL of alkaline activator was added per specimen to obtain a castable paste.

The fresh geopolymer paste was then poured into cube-shaped molds (5 × 5 × 5 cm). The filled molds were sealed to minimize moisture loss and cured at controlled temperatures of 30 °C, 60 °C or 90 °C. After curing, the specimens were demolded after 48 h, once sufficient hardening had occurred, and subsequently stored at room temperature until compressive strength testing.

### 2.3 Coal ashes and geopolymers characterization

The mineralogical composition of coal ashes was analyzed using petrographic analysis, X-ray diffraction (XRD), and geochemical analysis. Compressive strength tests were conducted at an age of 21 days to evaluate the stabilized mechanical performance of the geopolymer specimens after sufficient geopolymerization and microstructural development had occurred. This testing age was selected to ensure

reliable comparison among different mixture compositions, activator concentrations, and curing temperatures, while minimizing the influence of early-age strength fluctuations commonly observed in alkali-activated systems.

Chemical bonding in the geopolymer samples was evaluated using Fourier transform infrared spectroscopy (FTIR, Nicolet iS10, Thermo Fisher Scientific, USA). The aluminosilicate structure was interpreted based on FTIR absorption bands (Table 1) [18]. In addition, phase identification was conducted using X-ray diffraction (X'Pert PRO, PANalytical, Netherlands). The degree of geopolymerization was assessed using a correlation parameter (Corr) derived from FTIR spectra, based on spectral similarity with standardized zeolite [19]. The correlation coefficient *r* was calculated using Eq. (1), while the Corr value was determined using Eq. (2):

$$r = \frac{(a_i - \bar{a})(b_i - \bar{b})}{\sqrt{(a_i - \bar{a})^2 (b_i - \bar{b})^2}}, \quad (1)$$

$$\text{Corr} = \frac{(999(r + 1))}{2}. \quad (2)$$

where *a* and *b* are the spectral intensity values of the geopolymer sample and the reference zeolite at point *i*, respectively,  $\bar{a}$  and  $\bar{b}$  are their respective mean values, and *r* is the Pearson correlation coefficient. This parameter represents the similarity between the geopolymer sample and a reference aluminosilicate structure. Higher Corr values indicate a higher degree of geopolymerization and a more developed aluminosilicate network. This Corr parameter is consistently used throughout this study as a microstructural indicator and is not a correction factor applied to experimental data.

## 3 Results and discussion

For clarity, the geopolymer samples investigated in this study are designated based on their preparation method and storage condition. Samples labeled as Mixland refer to geopolymer specimens prepared and cured immediately after mixing under laboratory conditions, whereas samples labeled as Silo correspond to geopolymer specimens produced from raw materials that were stored prior to mixing.

The FA:BA mixing ratios and the origin of the raw materials (BPI, LA, and EN) are indicated consistently

**Table 1** The interpretation of aluminosilicate content in geopolymer characterization using FTIR data [18]

Wavelength (cm <sup>-1</sup> )	Functional group
900–1300	Si–O–T (T: Si, Al, tetrahedral) asymmetric stretching
1650	H–O–H bending
3400–3650	O–H symmetric and asymmetric stretching

throughout the results and discussion. To avoid ambiguity, the same sample designations are applied for all mechanical, microstructural, and physical property evaluations.

### 3.1 Coal ash characterization

The chemical composition of fly ash and bottom ash was determined using X-ray fluorescence analysis (XRF, PANalytical Axios, Malvern Panalytical, Netherlands). Fly ash and bottom ash were first characterized individually, and their combined characteristics were subsequently discussed within the context of the fly ash–bottom ash geopolymer system.

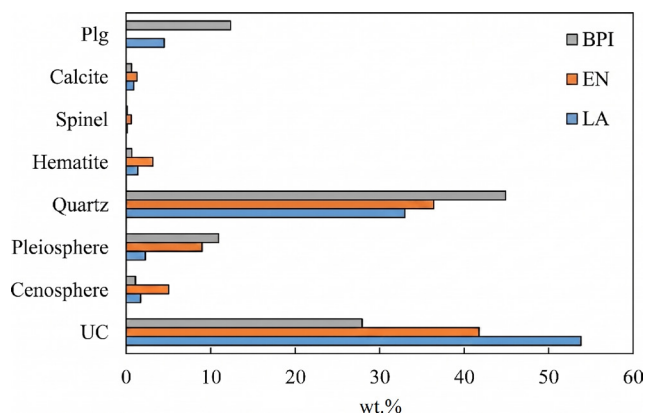
X-ray diffraction analysis was conducted on the raw materials to identify the crystalline phases present. The results confirm the presence of quartz, mullite, and iron oxide phases, consistent with the petrographic observations. For clarity, the XRD patterns are not shown separately, as the discussion focuses on the combined interpretation of petrographic and chemical analyses.

Petrographic analysis (Fig. 1 (a)) shows that the inorganic constituents of the fly ash and bottom ash samples consist mainly of glass, quartz, Fe-oxides, calcite, mullite, plagioclase and spinel, while unburned carbon (UC) represents the organic fraction. Quartz is the dominant inorganic phase in both materials. In the individual raw materials quartz contents range from approximately 17–75 wt.% in fly ash and 25–71 wt.% in bottom ash.

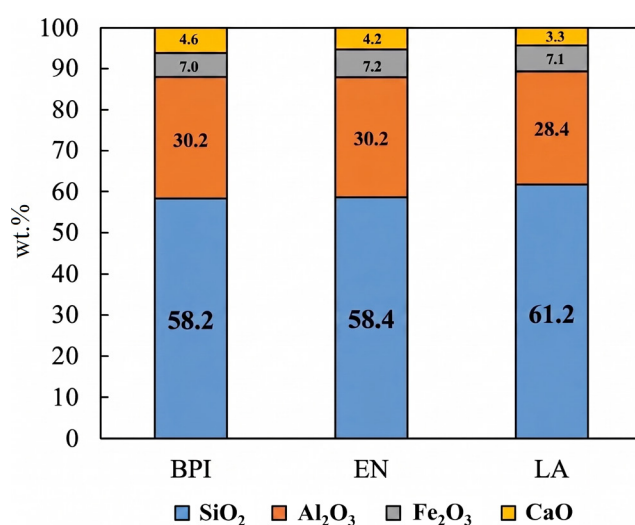
These values are semi-quantitative and are presented at an appropriate level of precision to reflect the limitations of the analytical methods. Quartz represents the crystalline  $\text{SiO}_2$  phase, whereas amorphous  $\text{SiO}_2$ -rich glass phases are also present and are typically identified morphologically as cenospheres and pleiospheres.

Although Fig. 1 (a) presents the petrographic features of the FABA, the quantitative phase contents of fly ash and bottom ash were determined separately from individual raw material analyses. Iron oxide minerals, predominantly magnetite ( $\text{Fe}_3\text{O}_4$ ), are present at levels of 0.56–7.91% in fly ash and 0.41–5.51% in bottom ash, based on quantitative phase analyses of the individual raw materials. Petrographic observations using polished sections reveal significant UC contents, indicating incomplete combustion. The UC content ranges from 12.50–76.30% in fly ash and 17.50–52.47% in bottom ash.

Mineralogical characterization of samples from the three power plants (Fig. 1 (b)) indicates that BPI contains the lowest amorphous silica content, ranging from 3.70–14.18%. EN exhibits the highest quartz abundance, reaching 73.93%,



(a)



(b)

**Fig. 1** Characterization of the fly ash–bottom ash system (FABA): (a) petrographic analysis; (b) major oxide composition determined by XRF

with UC content up to 60.28%, lower than LA but higher than BPI. In addition, EN shows the highest amorphous glass content (6.20–22.17%) and the highest Fe-oxide concentration, reaching 5.3%.

PLTU Lampung is characterized by quartz and UC as the dominant components in both fly ash and bottom ash, with UC reaching a maximum value of 76.05%, the highest among all investigated PLTUs. Conversely, PLTU BPI shows comparatively lower quartz content, with a maximum value of 49.51%. The characterization presented in this section focuses on the individual properties of fly ash and bottom ash obtained from the three coal-fired power plants. The term FABA is used here to describe the combined relevance of these materials as potential geopolymer precursors, rather than a specific mixture ratio. The effects of controlled FA:BA mixing ratios are systematically investigated in Section 3.2.

### 3.2 The effect of mixing ratio of fly ash:bottom ash (FA:BA) on compressive strength

The FA:BA mixing ratio plays a key role in determining the structural integrity of geopolymer concrete. In this study, FA:BA ratios of 100:0, 90:10 and 80:20 were investigated. Fig. 2 presents the compressive strength results

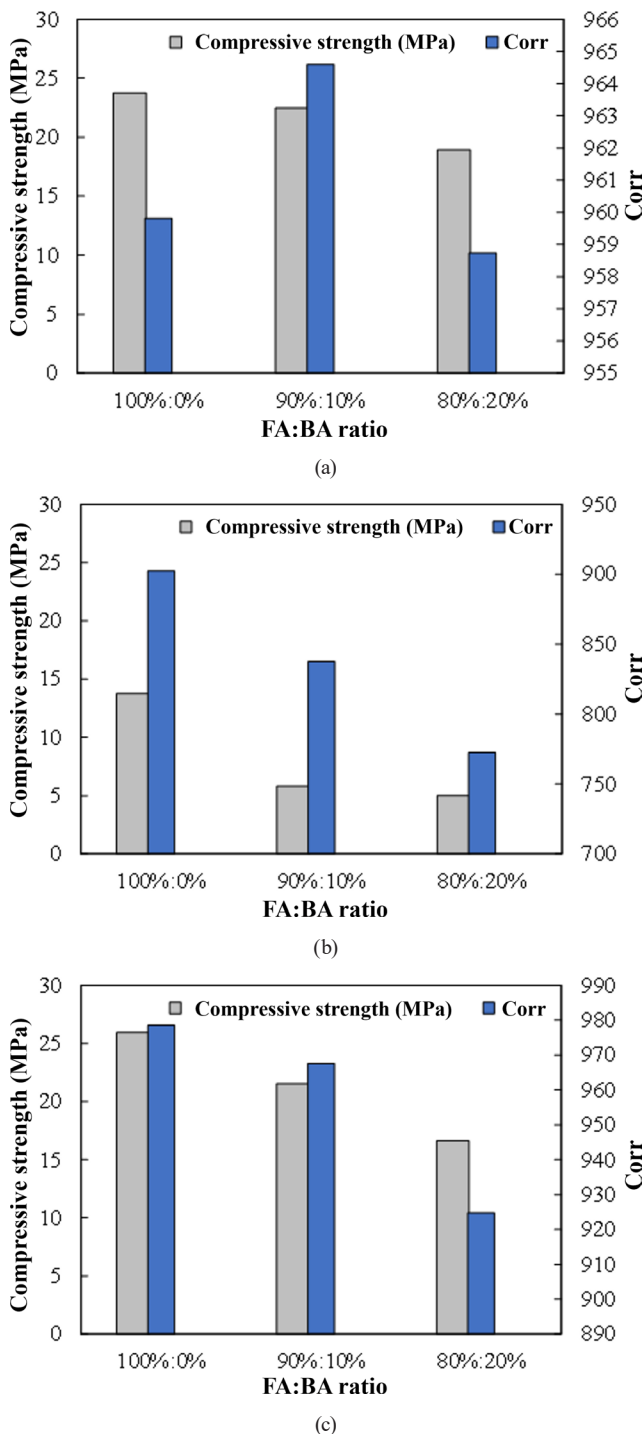


Fig. 2 Influence of FA:BA mixing ratio on compressive strength (grey bars) and compactness index (Corr, blue bars) for samples from: (a) BPI; (b) LA; (c) EN. Corr: FTIR-based correlation parameter indicating the degree of geopolymerization

for geopolymer samples derived from the three coal-fired power plants (Fig. 2 (a) to (c)). Overall, the inclusion of bottom ash significantly reduces compressive strength, and this trend is consistently observed across all samples, regardless of ash source.

In addition to compressive strength, the FTIR-derived correlation parameter is presented to provide insight into the degree of geopolymerization and microstructural development of each mixture. Corr is not used to normalize compressive strength values; rather, it serves as an independent microstructural indicator that complements the mechanical test results. As shown in Fig. 2, variations in Corr show a positive correlation with compressive strength, indicating that a higher degree of geopolymerization, as reflected by FTIR analysis, is associated with a more developed aluminosilicate network and higher mechanical strength. The compressive strength values presented are the original experimental results and were not normalized.

The decrease in compressive strength with increasing BA content is primarily attributed to the presence of coarse particles, which reduce surface area and weaken interparticle bonding within the geopolymer matrix. Geopolymerization is influenced not only by particle size but also by the Si, Al and Fe contents and the mineralogical composition of the precursor. The decomposition of minerals during alkaline activation depends strongly on the amorphous phase content [20]. Furthermore, coarse BA particles promote capillary pore formation, leading to reduced mechanical performance [21].

The results indicate that the coarser bottom ash particles do not actively participate in the geopolymerization process. Instead, bottom ash primarily acts as an inert filler, contributing to the composite structure rather than to geopolymeric gel formation, which is mainly governed by the finer fly ash fraction. This behavior is attributed to the lower reactivity and reduced surface area of the coarser bottom ash particles compared to fly ash.

### 3.3 The effect of curing temperature on compressive strength and its correlation with the Corr value

Temperature is a critical parameter in geopolymer concrete production due to its influence on the interaction between raw materials and alkaline activators. In this study, molding temperatures of 30 °C, 60 °C and 90 °C were applied. Fig. 3 illustrates the relationship between molding temperature and compressive strength.

For BPI, compressive strength increases consistently with temperature, reaching 19.27 MPa at 30 °C, 27.60 MPa

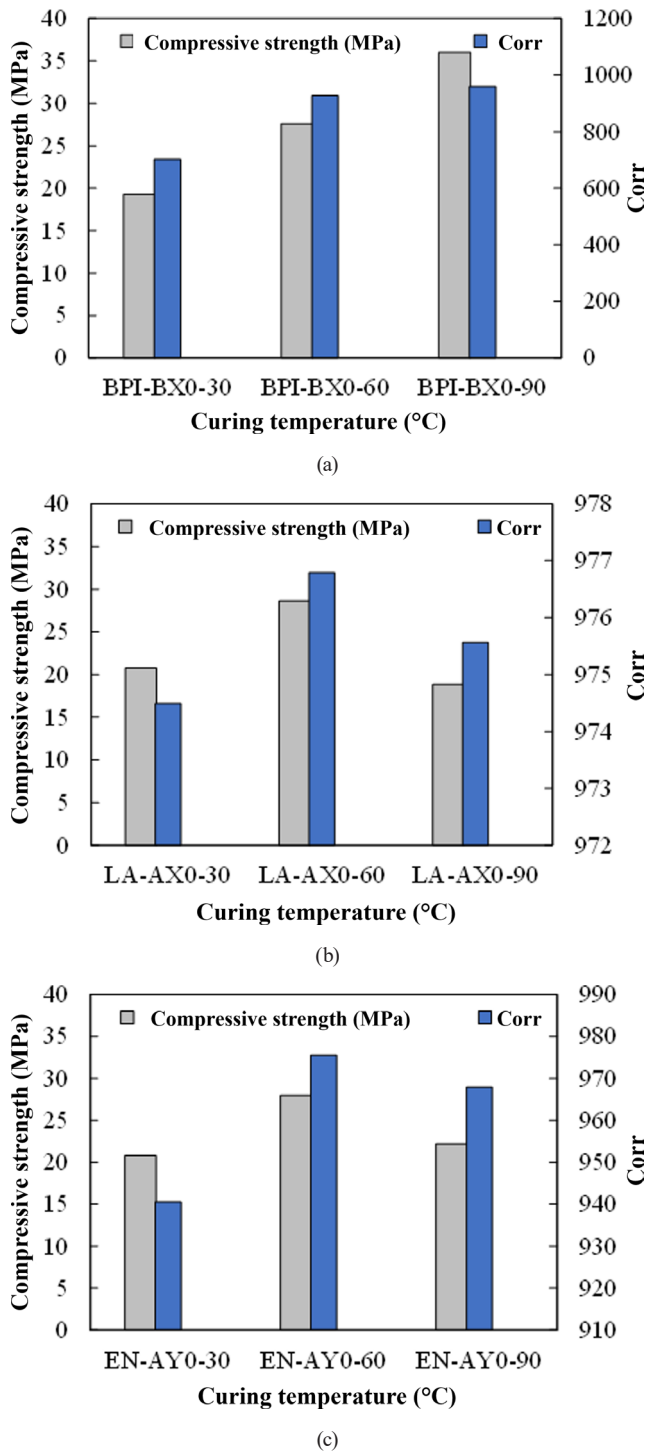


**Fig. 3** The influence of curing temperature on compressive strength: (a) BPI; (b) LA; (c) EN. Sample labels indicate the power plant origin (BPI, LA, EN) followed by the sample code and curing temperature (30, 60, or 90 °C). Corr: FTIR-based correlation parameter indicating the degree of geopolymerization

at 60 °C and 30.02 MPa at 90 °C, indicating nearly a two-fold increase compared to room temperature. EN shows an increase in compressive strength from 20.76 MPa at 30 °C to 28.60 MPa at 60 °C, followed by a decrease to

18.83 MPa at 90 °C. A similar trend is observed in LA, where compressive strength peaks at 60 °C before declining at 90 °C, with values of 20.80 MPa, 27.97 MPa and 22.21 MPa at 30 °C, 60 °C and 90 °C, respectively.

The increase in compressive strength at elevated temperatures is attributed to the endothermic dissolution of fly ash in NaOH, where external heat accelerates geopolymerization. However, excessive temperature (90 °C) promotes water loss and microcrack formation during molding, leading to reduced mechanical performance and increased brittleness during compressive strength testing [21].

### 3.4 The effect of unburned carbon on compressive strength

The presence of UC in fly ash directly affects the compressive strength of geopolymers, where higher UC content generally leads to lower strength. UC exhibits low reactivity with the geopolymer matrix and can induce crack formation after hardening, thereby inhibiting geopolymerization. As shown in Fig. 4 (a) to (c), a clear inverse relationship exists between UC content and compressive strength: as UC decreases, compressive strength increases. This trend is observed in almost all experimental results.

UC interferes with the geopolymerization process due to its preferential interaction with alkaline activators, which reduces the effective reaction between aluminosilicate phases and the activator [20]. Consequently, numerous studies recommend reducing UC content in fly ash prior to geopolymer production. Common approaches include high-temperature burning and froth flotation techniques [22]. Previous studies have consistently identified UC as an undesirable component in geopolymer materials [23], as it may also initiate corrosion when geopolymer concrete is exposed to water.

However, Fig. 5 (c) shows that the EN-FA-Coarse sample exhibits the lowest compressive strength despite having the lowest UC content. This anomaly is attributed to its nearly uniform particle size distribution, dominated by coarse quartz sand, which limits surface reactivity and weakens geopolymer bonding.

### 3.5 The effect of Si/Al ratio on compressive strength

The chemical composition of raw materials strongly influences the compressive strength of geopolymers. XRD and petrographic analyses show that SiO<sub>2</sub> is the dominant component in fly ash from all three PLTUs. SiO<sub>2</sub> plays a critical role in initiating oligomerization and polycondensation reactions during geopolymerization, thereby enhancing mechanical performance. The effect of SiO<sub>2</sub>

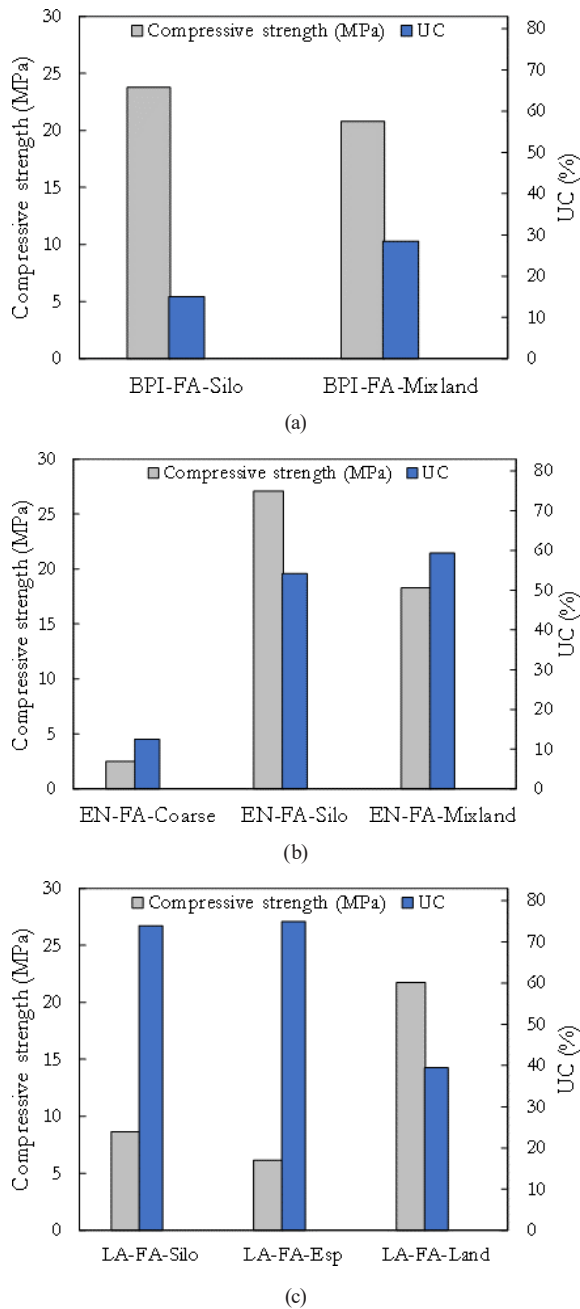


**Fig. 4** The influence of unburned carbon on compressive strength: (a) BPI; (b) LA; (c) EN

is commonly evaluated relative to  $\text{Al}_2\text{O}_3$  through the Si/Al ratio, which is known to govern geopolymer strength. A decrease in the Si/Al ratio generally leads to lower compressive strength due to the substitution of Si by Al, resulting in weaker Si–O–Al bonds compared to stronger Si–O–Si linkages. Consequently, compressive strength is directly correlated with the Si/Al ratio [24].

In this study, sample labels indicate the storage and collection conditions: 'Silo' refers to raw materials stored in a silo prior to mixing, 'Land' refers to materials collected from the landfill, 'Mixland' refers to landfill-collected materials mixed immediately after collection,

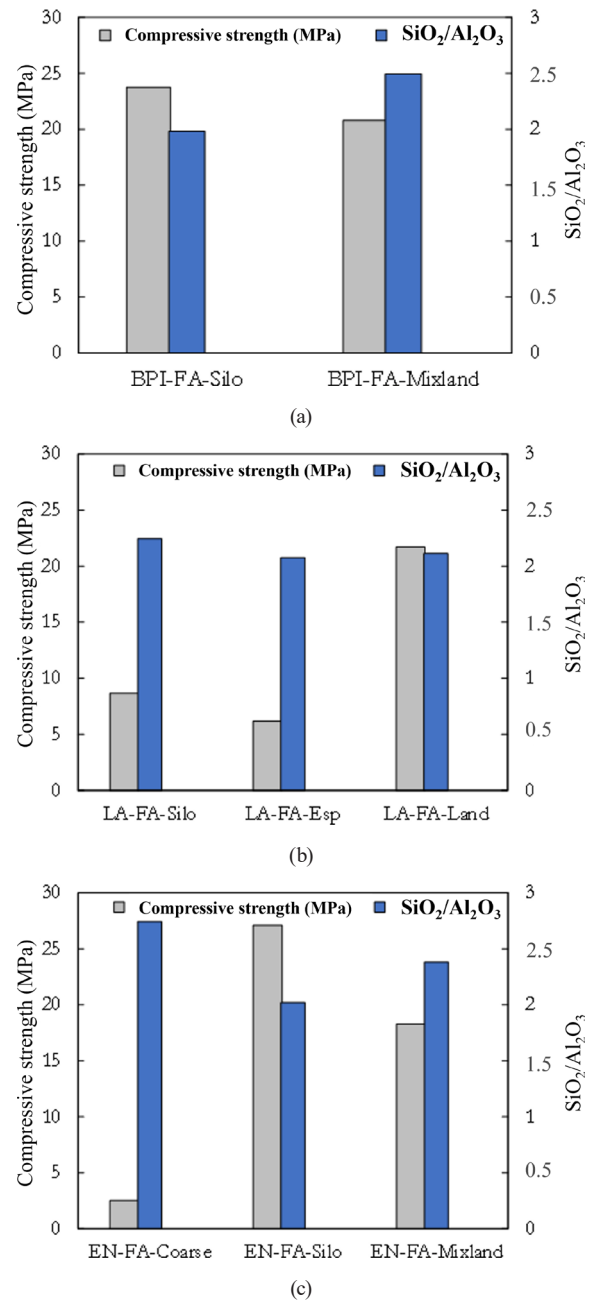


**Fig. 5** The influence of  $\text{SiO}_2/\text{Al}_2\text{O}_3$  ratio on compressive strength: (a) BPI; (b) LA; (c) EN

'Coarse' refers to fly ash with a coarse particle size fraction, 'Fresh' refers to bottom ash freshly collected from the ash pond, and 'Esp' refers to fly ash collected from the electrostatic precipitator. In the BPI samples (Fig. 5 (a)), BPI-FA-Silo and BPI-FA-Mixland exhibit  $\text{SiO}_2/\text{Al}_2\text{O}_3$  ratios of 1.98 and 2.49, respectively. Despite having a lower ratio, BPI-FA-Silo shows higher compressive strength, which is attributed to its lower  $\text{Fe}_2\text{O}_3$  content (5.37%) compared to BPI-FA-Mixland (6.23%). Elevated  $\text{Fe}_2\text{O}_3$  contents are known to inhibit geopolymerization and reduce compressive strength [25].

Fig. 5 (c) shows that EN-FA-Coarse possesses the highest  $\text{SiO}_2/\text{Al}_2\text{O}_3$  ratio but the lowest compressive strength. This behavior is attributed to its uniform medium-to-coarse particle size and dominance of crystalline silica, which limits surface reactivity. In contrast, EN-FA-Silo exhibits the highest compressive strength despite having a lower  $\text{SiO}_2/\text{Al}_2\text{O}_3$  ratio. This effect is associated with CaO content, which is 4.2%, 4.9%, and 4.06% for EN-FA-Coarse, EN-FA-Silo, and EN-FA-Mixland, respectively. Lower CaO contents delay early hardening, while higher CaO levels accelerate setting and promote silicate formation, leading to enhanced compressive strength [26].

### 3.6 The effect of activator concentration on compressive strength and its correlation with the Corr value

An activator is a chemical agent used to initiate geopolymerization by activating particle surfaces, thereby directly influencing the compressive strength of geopolymer concrete. Fig. 6 illustrates the effect of NaOH concentration on compressive strength for geopolymer concretes prepared from different fly ash sources.

NaOH concentrations of 6 M, 8 M, and 10 M were investigated. As shown in Fig. 6, increasing NaOH concentration from 6 M to 8 M significantly enhances compressive strength. The maximum compressive strengths at 8 M were 21.72 MPa for PLTU Lampung (FA Silo), 18.09 MPa for PLTU Enim (FA Silo), and 21.25 MPa for PLTU BPI (FA Silo). This improvement is attributed to enhanced dissolution of Si and Al species, which act as cementitious components and strengthen geopolymeric bonding [27].

However, further increasing NaOH concentration to 10 M results in reduced compressive strength. Excessive  $\text{OH}^-$  ions promote rapid dissolution of Si and Al but inhibit the polycondensation process [28]. High alkalinity also leads to early precipitation of aluminosilicate gels, prolonging the gel phase and delaying hardening [29]. Consequently, geopolymer concrete prepared with 10 M NaOH remains soft for up to 21 days and exhibits lower compressive strength.

### 3.7 FTIR-based microstructural insights and carbon footprint reduction of fly ash – bottom ash geopolymers

FTIR analysis indicates that the dominant bonds formed during geopolymerization are Si–O–Al and  $\text{OH}^-$  bonds. Fig. 7 presents the FTIR spectra of geopolymer samples from the three PLTUs prepared with FA:BA ratios of 100:0, 90:10, and 80:20 at a NaOH concentration of 8 M. For the LM samples (Fig. 7 (a)), FA-ESP without BA exhibits FTIR peak intensities approximately 10–20%

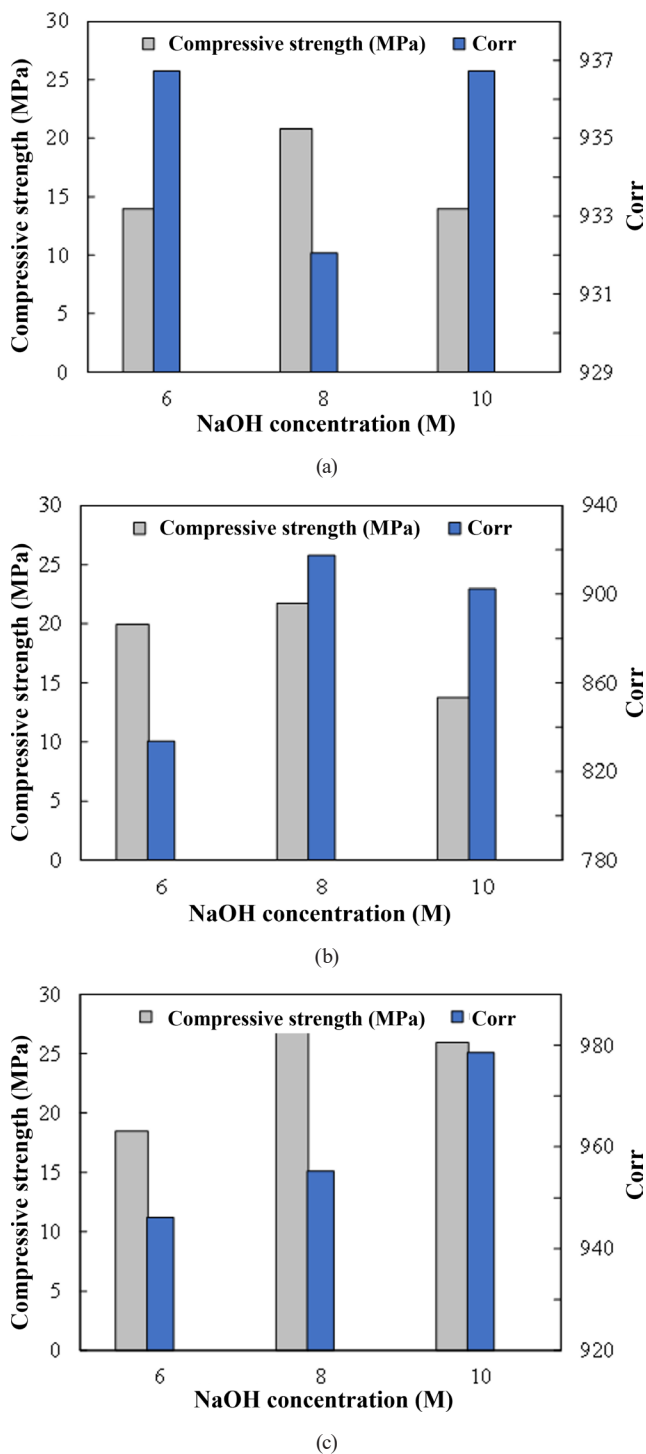
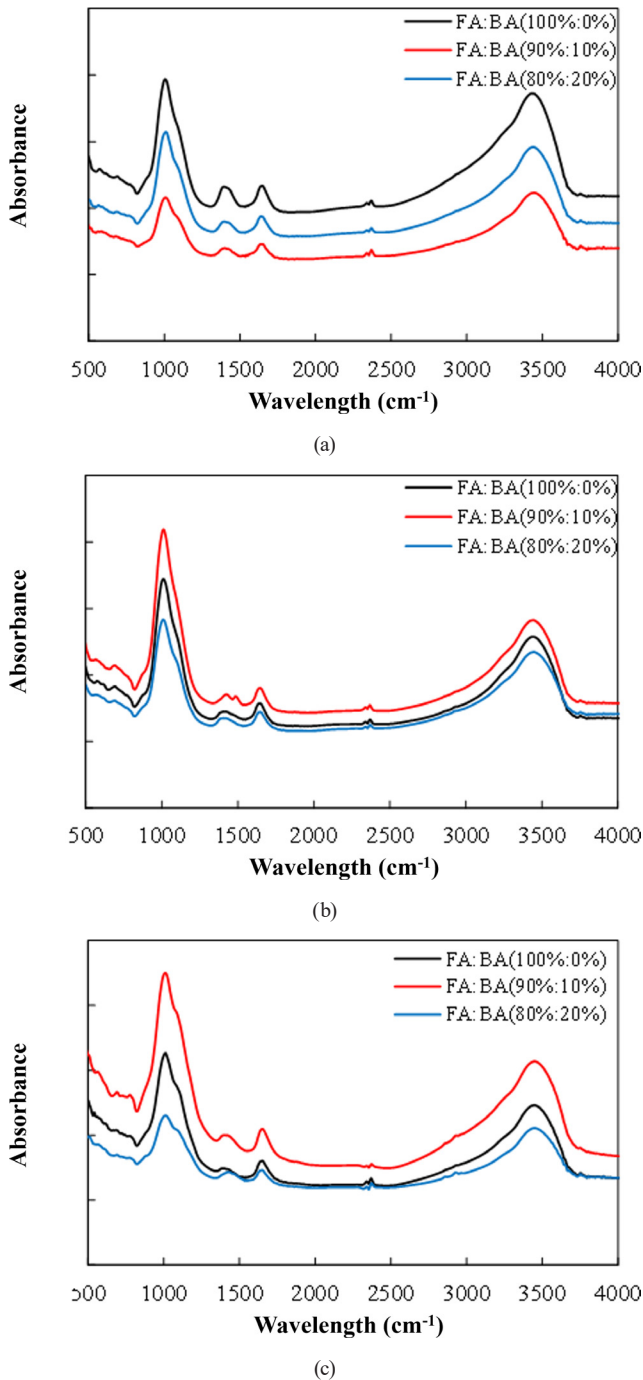


Fig. 6 The influence of sodium hydroxide concentration on compressive strength: (a) BPI; (b) LA; (c) EN

higher than those of samples containing BA-Land, particularly in the OH symmetric vibration region. Variations in this region influence compressive strength, indicating that water-related functional groups play a significant role in determining geopolymer performance.

In the EN samples (Fig. 7 (b)), FA-Silo with 10% BA-Fresh shows the highest FTIR intensity compared to the 0% and 20% BA mixtures; however, increasing FTIR



**Fig. 7** FTIR data analysis: (a) LM-FA-Esp. and BA-Land; (b) EN-FA-Silo and BA-Fresh; (c) BPI-FA-Silo and BA-Silo)

intensity corresponds to a reduction in compressive strength, with values of 27.09 MPa, 18.07 MPa, and 27.30 MPa for BA contents of 0%, 10% and 20%, respectively. Overall, FA-Silo-based geopolymers exhibit higher compressive strength due to the predominance of Si–O–Si and Si–O–Al bonds. For the BPI samples (Fig. 7 (c)), the FA:BA ratio 90:10 shows the highest asymmetric stretching vibration peak, indicating enhanced formation of Si–O–Si and Si–O–Al bonds; however, compressive strength differ-

ences among the mixtures are relatively small, reaching 23.77 MPa, 24.85 MPa, and 25.43 MPa for FA:BA ratios of 100:0, 90:10, and 80:20, respectively. In general, higher correlation (Corr) values indicate a greater degree of geopolymer conversion and higher compressive strength, while the addition of BA tends to increase OH<sup>-</sup> group intensity, reflecting higher water content, reduced microstructural density, and increased water absorption, which ultimately lowers compressive strength [30].

Beyond mechanical performance, the microstructural characteristics revealed by FTIR analysis are closely linked to the environmental advantages of geopolymer systems. Growing concern over the environmental impact of the construction industry has highlighted the high carbon dioxide emissions associated with ordinary Portland cement (OPC), whose production is highly energy-intensive. Fig. 8 compares the CO<sub>2</sub>-equivalent emissions from the production and construction of 1 m<sup>3</sup> of concrete using OPC and geopolymer with Sumatera FABA [31]. OPC exhibits emissions of 354 kg CO<sub>2</sub>-eq/m<sup>3</sup>, dominated by cement production (269 kg CO<sub>2</sub>-eq/m<sup>3</sup>, 76%), whereas geopolymer with Sumatera FABA emits 256 kg CO<sub>2</sub>-eq/m<sup>3</sup>, corresponding to a 27.7% reduction. This reduction is achieved primarily through the substitution of cement with industrial by-products such as fly ash (20 kg CO<sub>2</sub>-eq/m<sup>3</sup>) and bottom ash (18 kg CO<sub>2</sub>-eq/m<sup>3</sup>), despite the contributions from sodium silicate (100 kg CO<sub>2</sub>-eq/m<sup>3</sup>) and sodium hydroxide (25 kg CO<sub>2</sub>-eq/m<sup>3</sup>) as activators. Unlike OPC, which requires high-temperature kilns, geopolymers are synthesized at lower temperatures, leading to reduced energy consumption and emissions; this is particularly significant given that up to 55% of the carbon footprint of construction materials originates from production and construction stages [32]. In addition to lower emissions, geopolymers with Sumatera FABA exhibit

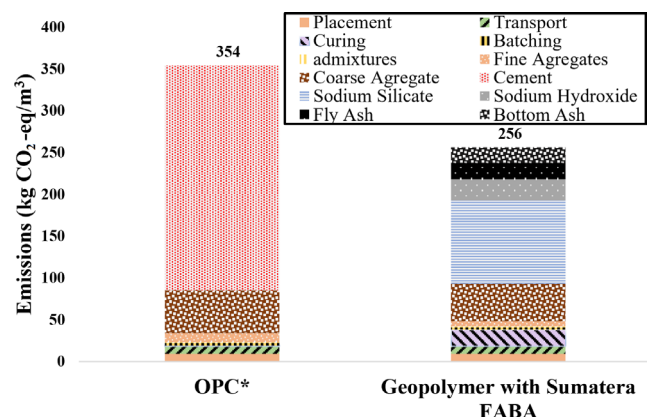


**Fig. 8** Analyzing CO<sub>2</sub> emission profiles of OPC and bottom ash-enhanced geopolymer (\* based on Turner et al. [31])

adequate mechanical performance, achieving compressive strengths of up to 27 MPa, while also enabling CO<sub>2</sub> capture through carbonation. The combination of favorable microstructural development, reduced carbon emissions, and effective utilization of industrial waste highlights the potential of FABA-based geopolymers as sustainable, circular-economy-oriented construction materials.

Compared to previous studies that primarily focus on single fly ash-based geopolymer systems, the present study demonstrates that the incorporation of bottom ash significantly alters both geopolymerization behavior and mechanical performance. While earlier works often report compressive strength trends based on individual parameters, such as activator concentration or curing temperature, this study highlights the combined effects of FA:BA ratio, NaOH concentration and curing temperature, revealing trade-offs between strength enhancement and microstructural stability. In addition, unlike many studies that treat fly ash as a uniform precursor, the results emphasize the influence of local ash characteristics, including unburned carbon content and mineralogical composition, on performance consistency. The FTIR-based correlation analysis further distinguishes this work by linking microstructural development directly to mechanical behavior, providing a more mechanistic interpretation of FABA-based geopolymer performance.

Future research should address durability performance, large-scale applicability, and variability in ash characteristics, as well as integrate life cycle and economic assessments to further evaluate the practical sustainability of FABA-based geopolymer systems.

#### 4 Conclusion

This study demonstrates that geopolymer concrete can be produced using fly ash and bottom ash (BA) from coal-fired

power plants in Sumatera, with compressive strength governed by material composition and processing conditions. The alkaline activator concentration was the most influential parameter, with 8 M NaOH yielding the highest compressive strengths of 21.72 MPa for LA-FA-Land, 27.09 MPa for EN-FA-Silo and 29.09 MPa for BPI-FA-Silo, while higher concentrations reduced strength due to excessive OH<sup>-</sup> ions. Increasing BA content decreased compressive strength because of coarse particles and increased porosity, while higher curing temperatures enhanced strength but caused microcracking at around 90 °C. Higher SiO<sub>2</sub> content and optimal Si/Al ratios improved strength, whereas elevated unburned carbon reduced performance by absorbing activators. FTIR analysis showed that stronger Si–O–Al and Si–O–Si networks and lower OH<sup>-</sup> intensity correspond to a denser microstructure and higher compressive strength. In addition to mechanical performance, the substitution of Portland cement with Sumatera FABA reduces CO<sub>2</sub> emissions by lowering energy intensive cement production and promoting industrial waste utilization, supporting sustainable construction.

#### Acknowledgement

The authors gratefully acknowledge Universitas Gadjah Mada (UGM), the Research and Development Division for Mineral Technology, Indonesian Research and Innovation Agency (BRIN), Lampung, Institut Teknologi Sepuluh Nopember (ITS), and PT Bukit Asam (PTBA) for their support, including the provision of fly ash samples and access to laboratory and analytical facilities. The authors also thank the technical staff and researchers for their valuable assistance throughout this study. The authors declare that there is no conflict of interest regarding the publication of this work.

#### References

- [1] Energy and Mineral Resources Ministry "Indonesia Electricity Development Plan and Indonesia Coal-Ash Management Implementation", In: International Coal Based Power Conference, New Delhi, India, 2016, pp. 4–8.
- [2] Ministry of Energy and Mineral Resources Republic of Indonesia "Handbook of Energy and Economic Statistic of Indonesia. Jakarta: Ministry of Energy and Mineral Resources Republic of Indonesia", [pdf] Ministry of Energy and Mineral Resources Republic of Indonesia, Jakarta, Indonesia, 2017. Available at: <https://www.esdm.go.id/assets/media/content/content-handbook-of-energy-economic-statistics-of-indonesia-2017-.pdf> [Accessed: 02 January 2026]
- [3] Adelizar, A. S., Olvianas, M., Adythia, D. M., Syafiyurrahman, M. F., Pratama, I. G. A. A. N., Astuti, W., Petrus, H. T. B. M. "Fly Ash and Bottom Ash Utilization as Geopolymer: Correlation on Compressive Strength and Degree of Polymerization Observed using FTIR", IOP Conference Series: Materials Science and Engineering, 742(1), 012042, 2020. <https://doi.org/10.1088/1757-899X/742/1/012042>
- [4] Timotius, D., Kurniawan, A., Istiani, A., Suryanaga, C. E., Fahrialam, A., ..., Anggara, F. "An economic analysis of a novel potassium humate (K-Humate) production process from low rank coal: Incorporating carbon capture and heat integration process", Journal of Cleaner Production, 522, 146316, 2025. <https://doi.org/10.1016/j.jclepro.2025.146316>

- [5] Guermiti, L., Guendouz, M., Boukhelkhal, D., Abid, S., Hadjadj, M. "Potential of Producing Lightweight Cork-Based Mortars Reinforced with Polyethylene Fibers for Building Applications", *Buildings*, 16(1), 102, 2026.  
<https://doi.org/10.3390/buildings16010102>
- [6] Murti Petrus, H. T. B., Adelizar, A. S., Widiyatmoko, A., Olvianas, M., Suprpta, W., Perdana, I., Prasetya, A., Astuti, W. "Kinetics of Fly Ash Geopolymerization using Semi Quantitative Fourier-Transform Infrared Spectroscopy (FTIR); Corr Data", *IOP Conference Series: Materials Science and Engineering*, 532(1), 012001, 2019.  
<https://doi.org/10.1088/1757-899x/532/1/012001>
- [7] Supriadi, H., Suyanti, S., Astuti, W., Handini, T., Sujoto, V. S. H., Prameswara, G. "Optimization and Kinetics of Terbium Leaching from Lapindo Mud using Sulfuric Acid as the Leaching Agent", *Bulletin of Chemical Reaction Engineering & Catalysis*, 20(1), pp. 35–43, 2025.  
<https://doi.org/10.9767/brec.20252>
- [8] Jyothi, R. K., Thenepalli, T., Ahn, J. W., Parhi, P. K., Chung, K. W., Lee, J.-Y. "Review of rare earth elements recovery from secondary resources for clean energy technologies: Grand opportunities to create wealth from waste", *Journal of Cleaner Production*, 267, 122048, 2020.  
<https://doi.org/10.1016/j.jclepro.2020.122048>
- [9] Ulandari, O., Sujoto, V. S. H., Astuti, W., Anggara, F. Petrus, H. T. B. M., Prasetya, A. "Enhancement of compressive strength in geopolymers: a study on fly ash characteristics and solid activation using dry method", *Journal of Material Cycles and Waste Management*, 27(4), pp. 2303–2320, 2025.  
<https://doi.org/10.1007/s10163-025-02233-4>
- [10] Hadjadj, M., Guendouz, M., Boukhelkhal, D. "The effect of using seashells as cementitious bio-material and granite industrial waste as fine aggregate on mechanical and durability properties of green flowable sand concrete", *Journal of Building Engineering*, 87, 108968, 2024.  
<https://doi.org/10.1016/j.jobee.2024.108968>
- [11] Conroy, G. "Global warming is on the cusp of crucial 1.5 °C threshold, suggest ice-core data", *Nature*, Nov. 12., 2024.  
<https://doi.org/10.1038/d41586-024-03655-0>
- [12] Abdel-Gawwad, H. A., Abo-El-Enein, S. A. "A novel method to produce dry geopolymer cement powder", *HBRC Journal*, 12(1), pp. 13–24, 2016.  
<https://doi.org/10.1016/j.hbrcj.2014.06.008>
- [13] Guo, X., Shi, H., Dick, W. A. "Compressive strength and micro-structural characteristics of class C fly ash geopolymer", *Cement and Concrete Composites*, 32(2), pp. 142–147, 2010.  
<https://doi.org/10.1016/j.cemconcomp.2009.11.003>
- [14] Brus, J., Abbrent, S., Kobera, L., Urbanova, M., Cuba, P. "Chapter Two - Advances in 27Al MAS NMR Studies of Geopolymers", In: Webb, G. A. (ed.) *Annual Reports on NMR Spectroscopy*, Elsevier, 2016, pp. 79–147. ISBN 978-0-12-804713-2  
<https://doi.org/10.1016/bs.arnmr.2015.11.001>
- [15] Phair, J. W., Van Deventer, J. S. J. "Effect of silicate activator pH on the leaching and material characteristics of waste-based inorganic polymers", *Minerals Engineering*, 14(3), pp. 289–304, 2001.  
[https://doi.org/10.1016/S0892-6875\(01\)00002-4](https://doi.org/10.1016/S0892-6875(01)00002-4)
- [16] Mohan Kumar, S. G. K., Kinuthia, J. M., Oti, J., Adeleke, B. O. "Geopolymer Chemistry and Composition: A Comprehensive Review of Synthesis, Reaction Mechanisms, and Material Properties—Oriented with Sustainable Construction", *Materials*, 18(16), 3823, 2025.  
<https://doi.org/10.3390/ma18163823>
- [17] Luukkonen, T., Abdollahnejad, Z., Yliniemi, J., Kinnunen, P., Illikainen, M. "One-part alkali-activated materials: A review", *Cement and Concrete Research*, 103, pp. 21–34, 2018.  
<https://doi.org/10.1016/j.cemconres.2017.10.001>
- [18] Król, M., Minkiewicz, J., Mozgawa, W. "IR spectroscopy studies of zeolites in geopolymeric materials derived from kaolinite", *Journal of Molecular Structure*, 1126, pp. 200–206, 2016.  
<https://doi.org/10.1016/j.molstruc.2016.02.027>
- [19] Varmuza, K., Karlovits, M., Demuth, W. "Spectral similarity versus structural similarity: infrared spectroscopy", *Analytica Chimica Acta*, 490(1–2), pp. 313–324, 2003.  
[https://doi.org/10.1016/S0003-2670\(03\)00668-8](https://doi.org/10.1016/S0003-2670(03)00668-8)
- [20] Lee, S., Seo, M.-D., Kim, Y.-J., Park, H.-H., Kim, T.-N., Hwang, Y., Cho, S.-B. "Unburned carbon removal effect on compressive strength development in a honeycomb briquette ash-based geopolymer", *International Journal of Mineral Processing*, 97(1–4), pp. 20–25, 2010.  
<https://doi.org/10.1016/j.minpro.2010.07.007>
- [21] Chindapasirt, P., Chareerat, T., Sirivivatnanon, V. "Workability and strength of coarse high calcium fly ash geopolymer", *Cement and Concrete Composites*, 29(3), pp. 224–229, 2007.  
<https://doi.org/10.1016/j.cemconcomp.2006.11.002>
- [22] Gray, M. L., Champagne, K. J., Soong, Y., Killmeyer, R. P., Maroto-Valer, M. M., Andrésen, J. M., Ciocco, M. V., Zandhuis, P. H. "Physical cleaning of high carbon fly ash", *Fuel Processing Technology*, 76(1), pp. 11–21, 2002.  
[https://doi.org/10.1016/S0378-3820\(02\)00006-1](https://doi.org/10.1016/S0378-3820(02)00006-1)
- [23] Ha, T.-H., Muralidharan, S., Bae, J.-H., Ha, Y.-C., Lee, H.-G., Park, K. W., Kim, D.-K. "Effect of unburnt carbon on the corrosion performance of fly ash cement mortar", *Construction and Building Materials*, 19(7), pp. 509–515, 2005.  
<https://doi.org/10.1016/j.conbuildmat.2005.01.005>
- [24] Mustofa, M., Pintowantoro, S. "The Effect of Si/Al Ratio to Compressive Strength and Water Absorption of Ferronickel Slag-based Geopolymer", *IPTEK Journal of Proceedings Series*, 2, pp. 167–172, 2017.  
<https://doi.org/10.12962/j23546026.y2017i2.2334>
- [25] Choi, S. C., Lee, W. K. "Effect of Fe<sub>2</sub>O<sub>3</sub> on the Physical Property of Geopolymer Paste", *Advanced Materials Research*, 586, pp. 126–129, 2012.  
<https://doi.org/10.4028/www.scientific.net/AMR.586.126>
- [26] Leonard Wijaya, A., Jaya Ekaputri, J., Triwulan "Factors influencing strength and setting time of fly ash based-geopolymer paste", *MATEC Web of Conferences*, 138, 01010, 2017.  
<https://doi.org/10.1051/mateconf/201713801010>
- [27] Chindapasirt, P., Jaturapitakkul, C., Chalee, W., Rattanasak, U. "Comparative study on the characteristics of fly ash and bottom ash geopolymers", *Waste Management*, 29(2), pp. 539–543, 2009.  
<https://doi.org/10.1016/j.wasman.2008.06.023>

- [28] Zuhua, Z., Xiao, Y., Huajun, Z., Yue, C. "Role of water in the synthesis of calcined kaolin-based geopolymer", *Applied Clay Science*, 43(2), pp. 218–223, 2009.  
<https://doi.org/10.1016/j.clay.2008.09.003>
- [29] Lee, W. K. W., van Deventer, J. S. J. "The effects of inorganic salt contamination on the strength and durability of geopolymers", *Colloids and Surfaces A: Physicochemical and Engineering Aspects*, 211(2–3), pp. 115–126, 2002.  
[https://doi.org/10.1016/S0927-7757\(02\)00239-X](https://doi.org/10.1016/S0927-7757(02)00239-X)
- [30] Panyas, D., Giannopoulou, I. P., Perraki, T. "Effect of synthesis parameters on the mechanical properties of fly ash-based geopolymers", *Colloids and Surfaces A: Physicochemical and Engineering Aspects*, 301(1–3), pp. 246–254, 2007.  
<https://doi.org/10.1016/j.colsurfa.2006.12.064>
- [31] Turner, L. K., Collins, F. G. "Carbon dioxide equivalent (CO<sub>2</sub>-e) emissions: A comparison between geopolymer and OPC cement concrete", *Construction and Building Materials*, 43, pp. 125–130, 2013.  
<https://doi.org/10.1016/j.conbuildmat.2013.01.023>
- [32] Halim, L. N., Ekaputri, J. J., Triwulan "The Influence of Salt Water on Chloride Penetration in Geopolymer Concrete", *MATEC Web of Conferences*, 97, 01002, 2017.  
<https://doi.org/10.1051/mateconf/20179701002>